Egyptian Geophysical Society
EGS Journal, Vol. 19, No. 1, 175-188 (2021)

STATISTICAL ANALYSIS OF AIRBORNE GAMMA RAY SPECTROMETRIC DATA OF G. UMM NAGGAT AREA, CENTRAL EASTERN DESERT, EGYPT

S.O. BOURGIEAA, S.H. ABD EL NABI and K.S. FARAG

Geophysics Department – Faculty of Science Ain Shams University – Cairo – Egypt
salembourgieaa@gmial.com, samihamed60@gmail.com, karamsamir@gmx.net

التحليل الإحصائى لبيانات أشعة جاما الطيفية الجوية لمنطقة جبل أم نجاة، وسط الصحراء الشرقية, مصر

الخلاصة: أظهر تحليل القياس الطيفي لأشعة جاما بإستخدام الأجهزة المحمولة جواً لمنطقة جبل أم نجاة، وسط الصحراء الشرقية، مصر، أن المعالجة الإحصائية لهذه البيانات فيما يتعلق بالوحدات الجيولوجية الفردية مفيدة في تحديد نطاقات وفرة اليورانيوم التى تعتبر أحد أهم أهداف هذه الدراسة، والتي يمكن الإشارة إليها كدليل على التشوه المعدنى (alteration mineral)، حيث تم إتباع ثلاث طرق لتحديد مواقع أماكن وفرة اليورانيوم. تتمثل الطريقة الأولى لتحديد الإنحرافات في حساب متوسط قيم اليورانيوم لكل وحدة من الوحدات الصخرية المختلفة ومقارنتها بمتوسط القيمة المعيارية فى القشرة الأرضية لكل نوع صخري للعثور على مناطق وفرة اليورانيوم, حيث وجد أن صخور جبل أم نجاة، جبل العنيجى وجبل أم بيسلا تمتلك قيماً متوسطة تزيد عن القيمة المعيارية لصخور الحمضية 4.89 ppm, 4.89 ppm, 5.37 ppm على التوالى. ثانيا، تحديد منطقة الوفرة الشاذة بناءً على حساب القيم الشاذة العالية القيمة التي تساوي أو تتجاوز على الأقل انحرافين معياريين عن قيم الوسط الحسابي المحسوب (X+3S) & (X+2S) لقياسات اليورانيوم، لنقطة واحدة في كل وحدة صخرية. وتم تحديد ثلاث مناطق ذات وفرة لليورانيوم المكافى. حيث أنه عند تطبيق هاتين الطريقتين تبين أن ثلاث مجموعات رئيسية ل (eU)، والتي تتطابق مع قيم (eU/eTh , eU/K) المرتفعة المرتبطة بجرانيت البيوتايت الحديث والتى تشمل: شمال جبل أم نجاة بسبب عملية ألباتيزيشن (albitization)، جبل أم بسيلا و جبل الأونيجي. ثالثًا، رسم قطاعات مجمعة لخطوط طيران مختارة لمناطق وفرة اليورانيوم الموضح بالطريقتين السابقتين لتسهيل متابعة استجابة المناطق الشاذة على القنوات الطيفية المختلفة بالإضافة إلى القناة الطبوغرافية. وقد تم تتبع هذه القطاعات من عدة خطوط طيران: حيث تُظهر معظم القطاعات أن قنوات مكافىء اليورانيوم، ونسبة مكافىء اليورانيوم لمكافىء الثوريوم، ونسبة مكافىء اليورانيوم للبوتاسيوم عالية. وتعتبر هذه المناطق ذات الأولوية الأولى للمتابعة الجيولوجية والجيوفيزيائية والجيوكيميائية الأرضية. علاوة على ذلك، تم العثور على علاقة وثيقة بين أماكن الصدوع السطحية في المنطقة وأماكن وفرة اليورانيوم. من هذا التحليل نستخلص أن أجسام الجرانيت الحديث في مجال التنقيب عن اليورانيوم هي أكثر المناطق الواعدة.

ABSTRACT: *The analysis of airborne gamma ray spectrometric measurement for G. Umm Naggat area, Central Eastern Desert, Egypt, has shown that statistical treatment of these data with respect to individual geological units is useful in outlining the provinces of uranium enchainment that may be indicated for alteration processes. Three ways were followed to outline and locate the uraniferous provinces. First way is to compare the average of each rock unit with published crustal average value. Second way construct by uranium anomaly map where the position and the quantity of deviations in units equal to the standard deviation from the mean for eU, eU/eTh and eU/K could be outlined. These two ways demonstrate three major groups of high eU values, which coincide with high eU/eTh and eU/K values, related to biotite younger granites of the three pluton, north of Umm Naggat pluton due to albitization process, Umm Bisilla pluton and El Unayji pluton. While the third way is confirmed by examining the profiling across these anomalous zones of (eU, eU/eTh and eU/K) values. Furthermore a close relationship was found between the surface fault traces in the area and the spatial distribution of the identified spectrometric abnormalities. The younger granites plutons for uranium prospecting which are considered the most promising according this analysis.*

1. Geological Setting of the Study area

The region of G. Umm Naggat is situated in Central Eastern Desert of Egypt, which is basically part of the Nubian shield of the Pre-Cambrian period and mostly covered by basement rocks. Granite hills in the study region have a less rounded shape with sharp incisions regulated by joints and fault patterns. The metasediments are differentiated by the development of low land and strong dissection into low hills. Their distribution is uneven and their relief and slope is relatively low. Metavolcanics typically form scattered conical peaks and separated ridges, the serpentinites have a fairly soft and massive appearance with steep slopes. Post-granite dykes are more resistant than intruded country rocks and tend to be pronounced ridges that cut through the intruded rocks disconcordantly (Sabet, 1961). Lithostratigraphic rocks are metavolcanics, metagabbros, granodiorites, biotite granites and albite granites, which have been documented in the G. Um Naggat area (Fig. 1).

The granite contacts steeply dip into the country rocks (60^0-80^0). On the northern side, many dome-shaped projections of up to 1 km in diameter complicate

the shape of the granite, creating favorable structures for extensive metasomatic alteration of the original granite and the development of ore mineralization (Sabet et al., 1976). Albitized granite is defined by a strongly altered zone, which extends in width between 50 and 250 m and length up to 7 km. There are a lot of alteration processes like albitization, greisenization, kaolinization and fluoritization associated with the albitized granite, especially along major sinistral faults striking in NW–SE direction (Gaafar, 2015).

2. Gamma Ray Spectrometry Technique

The Eastern Desert of Egypt, was surveyed by airborne spectrometric and magnetic gamma rays in 1984. The survey used a high-resolution 256-channel gamma ray spectrometer system (50.31) with sodium iodide (Na I) crystal detectors, obtained with a 1km flight line interval and a 120m terrain clearance. The survey was acquired by the Aero Service Division of the Western Geophysical Company of America.

3. Data Analysis and Interpretation

According to Saunders and Potts (1976), significant eU anomalies were defined in three ways as follows:

- Compare average of eU value of each rock unit with the crustal published average of it is type.
- Point Anomaly map.
- Stacked Profile cross anomalous zones.

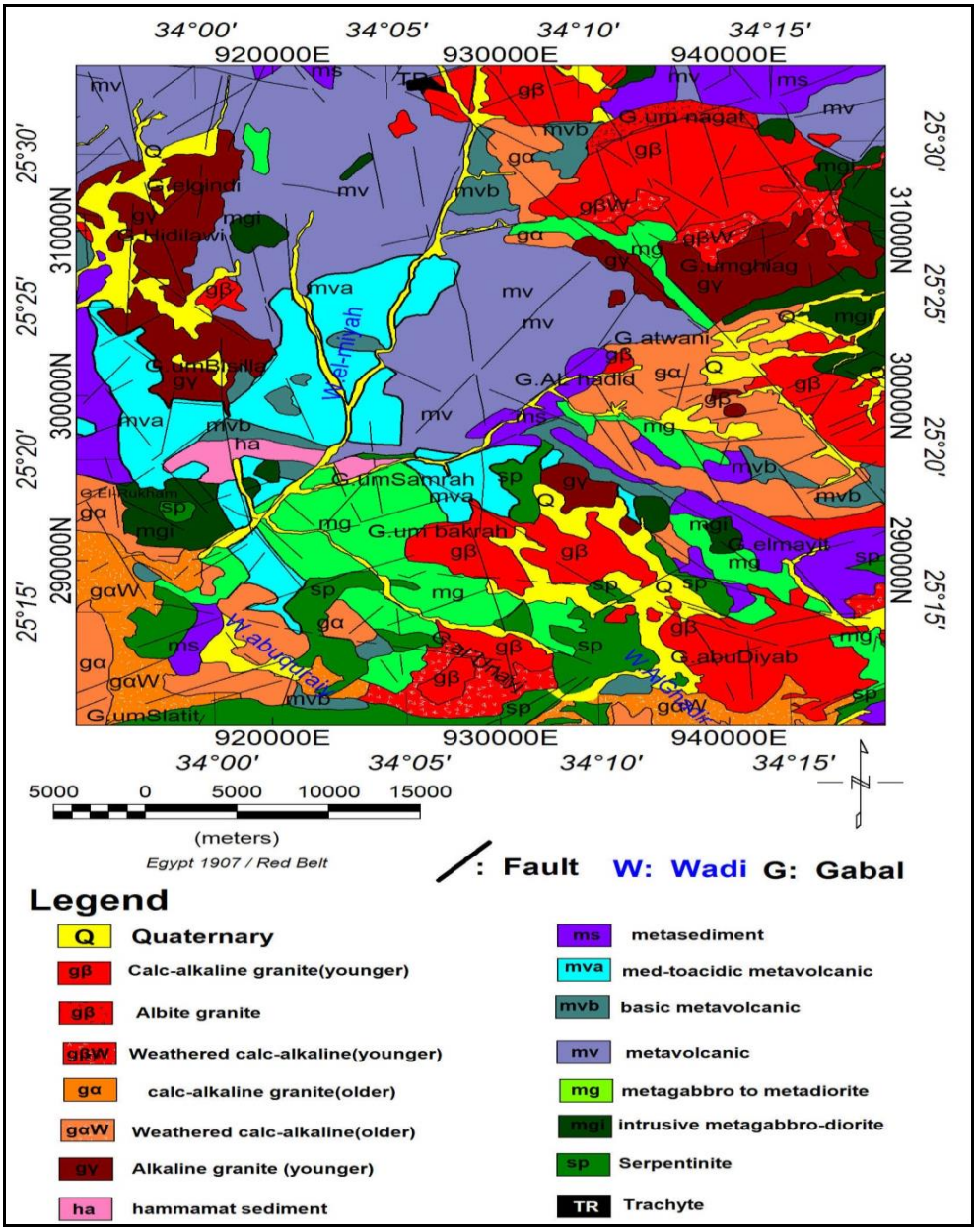

Fig. 1: Geologic map of Umm Naggat, Central Eastern Desert, Egypt (modified after Conoco, 1987).

3.1. Qualitative Analysis

3.1.1. Total Count

Total count contour map (Fig. 2) shows a wide variation of the measurements from one type of rock to another, and to more or less extent between the units of the same rock type. This wide variation reflects the fact that the mapped area is covered by rocks of various compositions. The investigation of this map displays a wide range of radioactivity values varying from about 0.1 to less than 75 (Ur). Generally, the TC map could be divided into four distinct zones according to the TC values, with overlapping Radioactivity levels. The highest radioactive zone has value ranged from 18.3 to 75 (Ur) and associated with three localities albite granite of G. Umm Naggat, G. Umm Bisilla and G. El Unayji. The second zone is associated with younger granite and values ranging between 11.6 to 18.3 (Ur). This level represented by many localities lying to the north of G. Umm Bisilla, G. El Hidilawi, scattered parts around G. El Jundi**,** W. Ghadir, G. Abu Diab, W. Umm Gheig and south of G. Umm Naggat.

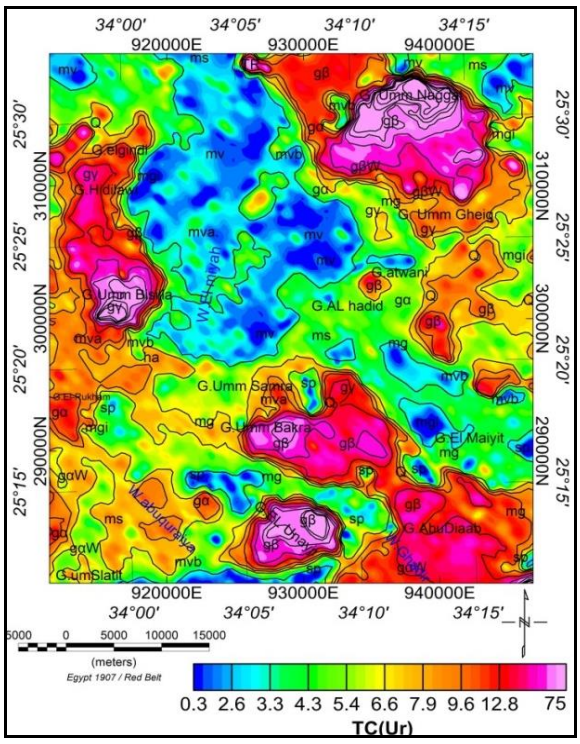

Fig. 2: Filled Color Total Count (TC) Contour Map of G. Umm Naggat, Central Eastern Desert, Egypt (After Aero Service, 1984).

All of these localities associated mainly with grey granite, coarse-grained biotite granite, and muscovite granite. It is noticeable that the contours or closures which formed this zones are aligned in a nearly NW- SE direction. The third zone values ranges from 5.8 to 11.6 (Ur). This level extends all over the southwestern and northeastern parts of the study area. Besides, it is represented by separate localities lying to the around G. El Jundi and G. Umm Gheig and north of G. El Hidilawi, as well as some other places of limited areal extent at the extreme southeastern portion of the study area. All of these localities are associated mainly with acidic metavolcanics, wadi sediments, metagabbro-diorite complex and grey granites. The forth zone values ranges from 0.3 to 5.8 (Ur). This level represents the lowest radioactivity level recorded in the study area. It extends over the northwestern and central parts of the study area up to the south of G. El Maiyit (Fig. 2). The range of radioactivity of this level is decreasing toward the center near W. El Miyah and It is associated mainly with serpentinites, basic metavolcanics and Metasediments.

3D visualization of total count map (Fig. 3) emphasize the anomalous zones of albite granite of Umm Naggat , G. Umm Bisilla, and G. El Unayji plutons.

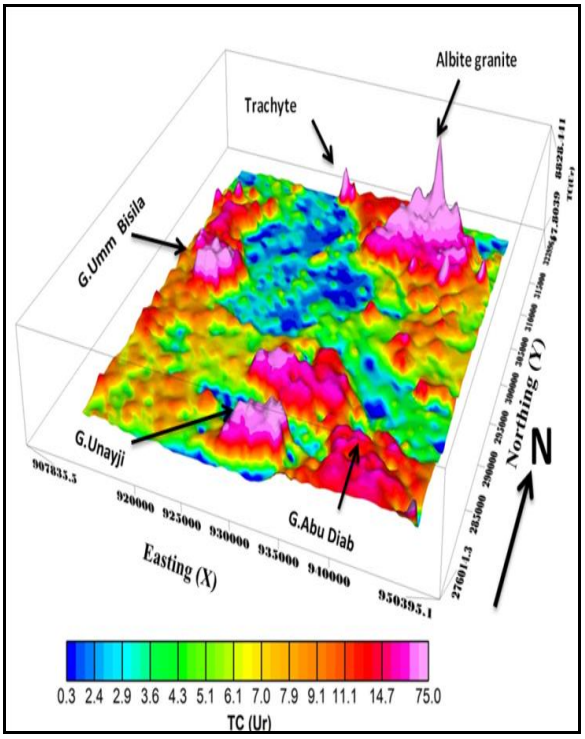

Fig. 3: 3D View of Total Count Map , of G. Umm Naggat, Central Eastern Desert, Egypt (After Aero Service, 1984).

3.1.2. Equivalent Uranium (eU) contour map.

Equivalent uranium colored contour map (Fig. 4) shows three uranium concentration levels according to their uranium contents. The first zone possess the most higher concentration where it is values ranges from 3 to 38.1 ppm (eU), and it is associated with north border of Umm Naggat pluton, the most of medium grained younger grnite in the area such as G. Umm Bisilla, G. Umm Bakra, G. El Unayji, the south of G. Umm Naggat. Second zone has moderate conecetration level with values ranges from 1.5 to 3 ppm (eU). This level

extends over the southwestern and northeastern parts of the study area. Besides, it is represented by separate localities lying around G. El Jundi and G. Umm Gheig and north of G. El Hidilawi, as well as some other places of limited areal extent at the extreme southwestern portion of the study area at G. Umm Salatit, W. Abu Quraiya and north of G. El Rukham. All of these localities are associated mainly with acidic metavolcanics, W. sediments, metagabbro-diorite complex and grey granites. The third zone has low conecetration level with values ranges from 0.1 to 1.5 ppm (eU). It extends over the northwestern and central parts of the study area up to the south of G. El Maiyit. The range of radioactivity of this level is decreasing toward the center of the mapped area near W. El Miyah. and It is associated mainly with serpentinites, basic metavolcanics and Metasediments.

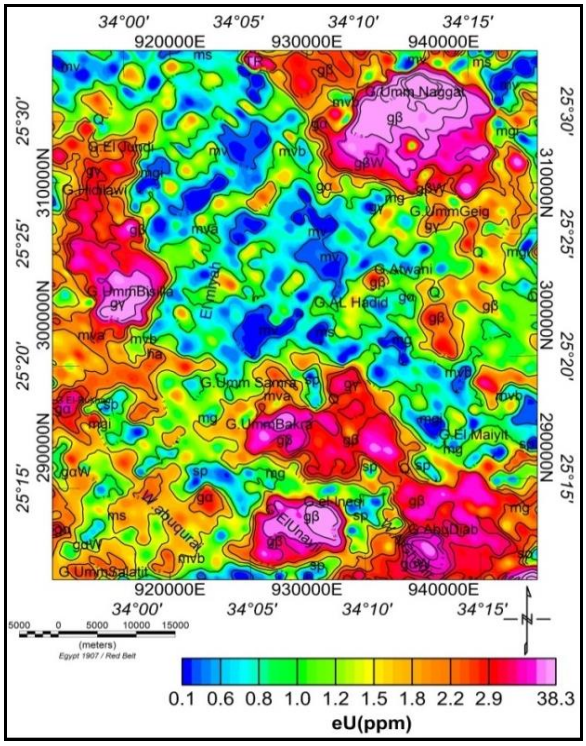

Fig. 4: Filled Color Equivalent Uranium (eU) Contour Map of G. Umm Naggat Central Eastern Desert, Egypt. (After Aero Service, 1984).

3.1.3. Potassium (K%) Contour Map.

The careful examination of the K % colored contour map (Fig. 5), reflects three levels of potassium concentrations. The highest K values constituting the first level from 2.6 to 3.81 % and associated mainly with the younger granite of Umm Naggat pluton zone as well as associated with coarse to medium grained biotite granites of G. Umm Bakra, G. El Unayji, and most of G. Abu Diab, G. El Hidilawi and G. Umm Bisilla, while the second zone values ranges from 1.2 to 2.6 and it is associated with the most of G. El Jundi in the western north, alluvial sediment around G. El Hidilawi, G. Umm Samra in the middle of the study area and G. Umm Gheig in the north east. Third zone values ranges from 0.2 to 1.2. It is occupied the middle of the mapped area extended NW- SE direction and associated with serpentinites, basic metavolcanics and Metasediments.

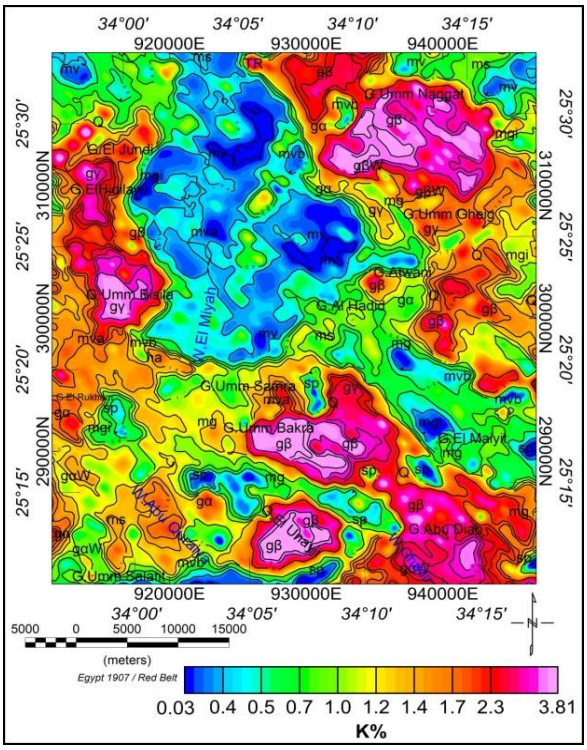

Fig. 5: Filled Color Potassium (K%) Contour Map of G. Umm Naggat Area, Central Eastern Desert, Egypt (after Aero Service 1984).

3.1.4. Equivalent Thorium (eTh) contour map.

Equivalent thorium colored contour map (Fig. 6) shows four thorium concentration levels depending on their thorium contents. The first zone has the most higher concentration level where it is values ranges from 13 to 56 ppm (eTh) associated with north of granitic pluton of Umm Naggat as Albite granite, and to the most of medium grained younger granite in the area such as G. Umm Bisilla pluton, G. Umm Bakra pluton, G. El Unayji pluton, the biotite granite of G. Umm Naggat pluton. Second zone has moderate conecetration level with values ranging from 7 to 13 (ppm). This level extends over the southwestern and northeastern parts of the study area at G. Abu Diab, G. El Jundi and El Hidilawi. Besides, it is associated with separate localities lying to the northwest of G. Umm Naggat. All of these localities are associated mainly with grey granite, coarse-grained biotite granite, wadi sediments, and metagabbro-diorite complex. The third zone values ranging from 4 to 7.0 (ppm). This level extends over the southwestern and northeastern parts of the study area. In the southwestern part where W. Abu Quraiya and south and east of G. Umm Bisilla and northeastern parts of the study area where G. and W. Umm Gheig, and part of G. Atwani. Besides, it is represented by

separate localities lying to the north of G. El Maiyit and W. El Miyah. All of these localities are associated mainly with acidic metavolcanics, wadi sediments, metagabbro-diorite complex and grey granites. The forth zone has values ranges from 0.1 to 4 (ppm) and represents the lowest radioactivity level recorded in the study area. It extends over the northwestern and central parts of the study area up to the south of G. El Maiyit (Fig. 6). The range of radioactivity of this level is decreasing toward the center near of the mapped area at W. El Miyah. and It associated mainly with serpentinites, basic metavolcanics and metasediments.

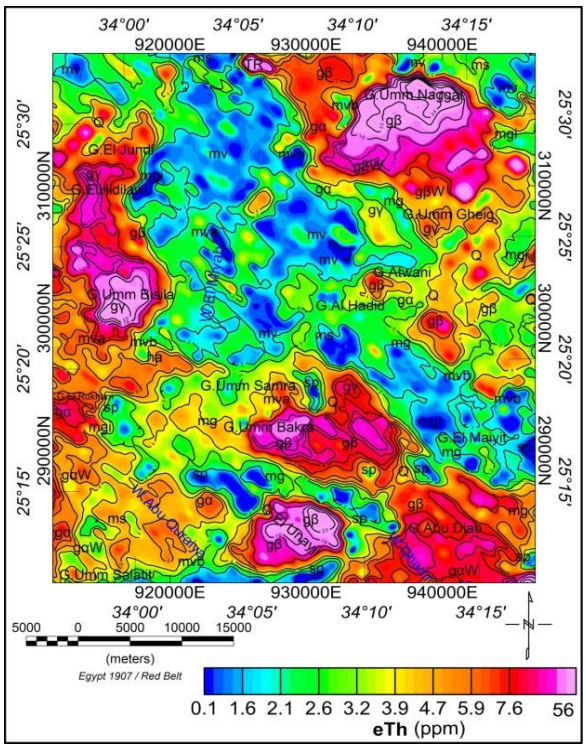

Fig. 6: Filled Color Equivalent Thorium (eTh) Contour Map of G. Umm Naggat Area, Central Eastern Desert, Egypt (after Aero Service 1984).

3.1.5. Equivalent Uranium/Thorium (eU/eTh) Ratio Contour Map:

The careful examination of equivalent uranium / equivalent thorium (eU/eTh) map (Fig. 7) shows that, the distribution of the eU/eTh values are spread over most geologic units, in the form of dispersed anomalies scattered in intermediate eU/eTh background. The lowest value which less than 0.38 (blue to green) as recorded in the study area are associated with metavolcanics, metasediments, ophiolitic metagabbro, metavolcanic, older granitic rocks and small parts of younger granitic rocks found as scattered spots in all area. Meanwhile, the highest value which reached to 3.4 (magenta color) are associated with albite granite alteration zone small parts of basic metavolcanic and intrusive metagabbro-diorite.

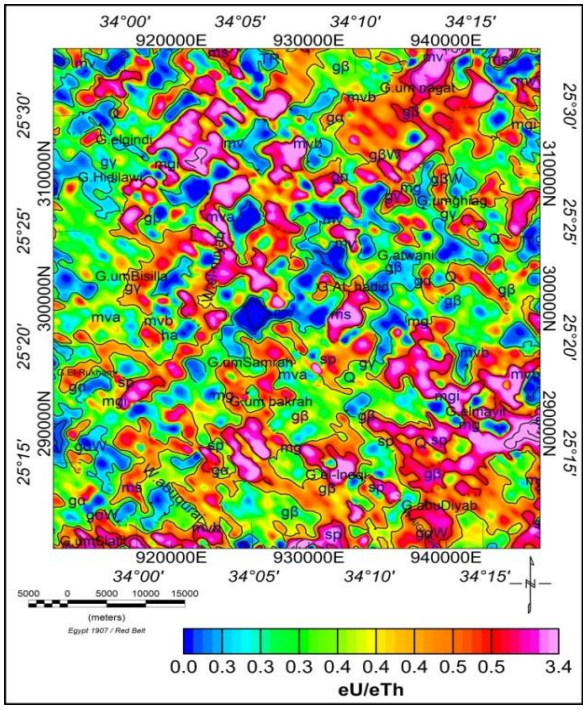

Fig. 7: Filled Color (eU/eTh) ratio Contour Map of G. Umm Naggat Central Eastern Desert of Egypt. (After Aero Service, 1984).

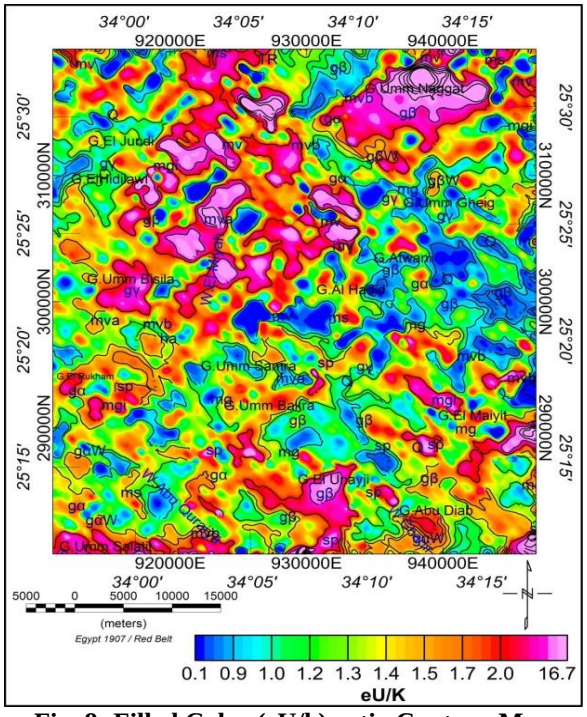

Fig. 8: Filled Color (eU/k) ratio Contour Map of G. Umm Naggat Area, Central Eastern Desert, Egypt (after Aero Service 1984).

3.1.6. Equivalent Uranium/Potassium (eU/K) Ratio Contour Map:

Equivalent uranium /potassium (eU/K) ratio contour map (Fig. 8) shows three levels of the ratios, the most higher ratio where associated with albite granite of G. Umm Naggat which it is values ranges from 7.3 to

16.73. While the middle values ratio ranges (2 - 7.3) associated with biotite granite of G. Umm Naggat, G. Umm Bakra, metavolcanic and metasediment of north of W. El Miyah up to the upper north of the study area.

Finally, the low values of eU/K are confined between (0.13-2) associated with most of the mapped area in the form dispersed spots of ophiolitic basic metavolcanics, metavolcanics, metasediments, ophiolitic metagabbro and granitic rocks.

3.2. Quantitave analysis.

The main objective of interpreting airborne gamma spectrometer data is to define the probable boundaries of the promised uraniferous anomalous provinces in which rocks and soils are preferably enriched with uranium (Saunders and Potts, 1976). This description could be based on groupings, considerable uranium anomalies or areas where the statistical characteristics of the data show that geochemical processes have selectively concentrated uranium in possible economic deposits (Abd El-Nabi,1995). The statistical treatment of gamma ray spectrometric data with respect to individual geological units was performed on digitized profiles along the traverse lines (Abd El-Nabi,1995).

According to Saunders and Potts (1976), significant eU anomalies were defined in three ways as follows:

- Compare the background mean of each rock unit with the published crustal average value for each rock type involved to find uranium-enriched units.
- By searching the uranium point anomaly map for grouping the statistically high points.
- By examining the stacked profiles for the regions of high eU, eU/eTh and eU/K values.

The first way of defining anomalies is by measuring the average uranium values for each of the various rock units and comparing them with the published crustal average value for each rock type involved to find uranium-enriched units. (Table 1) shows the mean eU, eTh and K values calculated for the prevailed rock units. Uranium values of 4.5, 2.3 and 1.0 ppm are typical average values for acidic, intermediate and basic igneous rocks, respectively (IAEA, 1979). A comparison of the calculated uranium average for each rock unit with its corresponding crustal average (Table1) shows that the younger granites of the three plutons Umm Naggat , Umm Bisilla and El Unayji have uranium values 5.37, 4.96 and 4.89 ppm respectively, exceed the crustal average of acidic rocks.

(Fig. 6) shows representative graph of K (%), eU (ppm) and eTh (ppm) with blue , red , and green color graph respectively. The peak of three graphs of K (%) , eU (ppm) and eTh (ppm) are associated with younger granites of G. Umm Naggat , G. El Unayji and G. Umm Bisilla

The second way to define significant eU anomalies is to classify certain areas where the eU values are more than three standard deviations above the mean for single-point, along with the local enrichment of eU over eTh and K (statistically high eU/eTh and eU/K ratio values). The deviations are expressed in units equal to the standard deviation of the appropriate data set for each of the prevailing rock units in G. Umm Naggat area (Table 2) & (Fig. 7).

Table 1: Calculated background mean (X) of radioelements, for the different rock units of G. Umm Naggat area, Central Eastern Desert, Egypt.

Rock Unit	eU (ppm)	eTh (ppm)	K%
Hammamat Sediment	1.8	3.49	1.33
Volcanic Group	1.11	2.92	0.71
MetaSediment	1.6	3.68	0.96
Umm Naggat younger granite	5.37	11.91	2.51
El Unayji younger granite	4.89	12.23	2.63
Umm Bisilla younger granite	4.96	13.53	2.74
El Hidilawi younger granite	2.34	7.38	1.93
umm Samra Umm Bakra younger granite	3.68	9.56	2.93
Umm Gheig younger granite	1.58	4.48	1.48
Abu Diab younger granite	3.44	7.43	2.36
Abu Quraiya older granite	1.81	4.97	1.3
Al Ghadir older granite	3.26	7.44	2.27
El Hadid older granite	1.28	3.43	1.18
Umm Naggat older granite	2.2	6.35	1.85
Mafic MetaGabbro Group	1.47	3.51	1.03
Ultramafic Serpentinite	1.4	3.11	0.84

Table (2): Statistical analysis of the variables in different geologic rock unit of G. Umm Naggat Area, Central Eastern Desert, Egypt.

Rock Unit	Variable	Count	Min	Max	Mean	Std. Dev.	(X+1S)	(X+2S)	(X+3S)
Older granite (gα)	TC (Ur)	616	2.43	18.97	7.58	2.91	10.49	13.40	16.31
	eU (ppm)		0.29	7.56	1.66	0.81	2.48	3.29	4.10
	eTh (ppm)		1.19	13.71	4.52	1.93	6.45	8.38	10.31
	k%		0.44	2.86	1.36	0.50	1.87	2.37	2.88
	eU/eTh		0.14	0.89	0.38	0.10	0.48	0.58	0.68
	eU/k		0.38	3.25	1.24	0.42	1.66	2.08	2.49
	eTh/k		1.37	6.94	3.33	0.79	4.12	4.91	5.70
Weathered plder granite (gαW)	TC (Ur)	261	4.49	16.12	9.01	3.35	12.36	15.70	19.05
	eU (ppm)		0.46	5.02	2.15	1.00	3.15	4.15	5.15
	eTh (ppm)		2.51	10.56	5.56	1.90	7.46	9.36	11.26
	k%		0.65	3.07	1.56	0.66	2.22	2.87	3.53
	eU/eTh		0.12	0.71	0.38	0.11	0.49	0.60	0.70
	eU/k		0.42	2.91	1.40	0.41	1.80	2.21	2.61
	eTh/k		2.39	7.04	3.71	0.70	4.41	5.11	5.82
Younger granite (gβ)	TC (Ur)	1007	1.97	62.04	15.44	7.07	22.51	29.58	36.65
	eU (ppm)		0.37	32.72	4.37	3.45	7.82	11.27	14.72
	eTh (ppm)		0.97	49.21	9.87	6.25	16.11	22.36	28.61
	k%		0.28	3.85	2.44	0.74	3.18	3.92	4.66
	eU/eTh		0.18	0.87	0.43	0.09	0.52	0.61	0.70
	eU/k		0.38	12.77	1.74	1.28	3.01	4.29	5.57
	eTh/k		1.26	19.62	3.96	2.15	6.11	8.26	10.40
Younger granite (gβW)	TC (Ur)	174	1.61	26.34	13.34	5.81	19.14	24.95	30.75
	eU (ppm)		0.59	8.22	3.34	1.83	5.17	7.00	8.83
	eTh (ppm)		0.68	22.41	8.57	4.52	13.09	17.62	22.14
	k%		0.28	3.60	2.19	0.82	3.01	3.83	4.66
	eU/eTh		0.25	0.88	0.40	0.08	0.47	0.55	0.62
	eU/k		0.64	2.68	1.48	0.42	1.90	2.31	2.73
	eTh/k		2.08	6.69	3.75	0.91	4.66	5.57	6.48
Younger granite (gγ)	TC (Ur)	508	3.94	30.43	12.03	5.38	17.41	22.78	28.16
	eU (ppm)		0.46	9.66	2.78	1.72	4.49	6.21	7.93
	eTh (ppm)		1.95	23.98	7.88	4.49	12.37	16.86	21.35
	k%		0.74	3.58	1.99	0.65	2.64	3.28	3.93
	eU/eTh		0.14	0.64	0.36	0.07	0.43	0.50	0.58
	eU/k		0.42	3.47	1.33	0.44	1.77	2.22	2.66
	eTh/k		2.02	7.70	3.77	1.06	4.82	5.88	6.93
Hammamat Clastics (ha)	TC (Ur)	48	4.10	10.91	7.99	1.67	9.66	11.33	13.00
	eU (ppm)		0.60	2.90	1.90	0.63	2.54	3.17	3.80
	eTh (ppm)		2.18	8.37	5.12	1.34	6.46	7.79	9.13
	k%		0.80	1.77	1.35	0.24	1.60	1.84	2.08
	eU/eTh		0.22	0.55	0.37	0.08	0.45	0.54	0.62
	eU/k		0.66	1.98	1.37	0.30	1.68	1.98	2.28
	eTh/k		2.73	5.52	3.75	0.57	4.31	4.88	5.44
Metagabbro-diorite (mg)	TC (Ur)	546	0.66	19.54	6.04	2.72	8.76	11.47	14.19
	eU (ppm)		0.21	7.17	1.47	0.84	2.31	3.15	3.99
	eTh (ppm)		0.21	16.28	3.43	1.76	5.19	6.95	8.70
	k%		0.10	3.25	1.07	0.48	1.55	2.02	2.50
	eU/eTh		0.15	3.52	0.47	0.26	0.72	0.98	1.24
	eU/k		0.53	5.00	1.43	0.56	1.99	2.55	3.10
	eTh/k		0.50	11.20	3.25	0.90	4.16	5.06	5.96

Rock Unit	Variable	Count	Min	Max	Mean	Std. Dev.	(X+1S)	(X+2S)	(X+3S)
Intrusive Metagabbro-diorite (mgi)	TC (Ur)	282	0.55	23.31	6.21	3.21	9.43	12.64	15.86
	eU (ppm)		0.24	8.50	1.58	1.22	2.79	4.01	5.22
	eTh (ppm)		0.90	20.15	3.98	2.64	6.63	9.27	11.91
	k%		0.13	2.49	1.05	0.43	1.47	1.90	2.32
	eU/eTh		0.15	0.90	0.41	0.14	0.55	0.69	0.84
	eU/k		0.54	6.27	1.56	0.85	2.41	3.26	4.11
	eTh/k		1.75	10.11	3.83	1.30	5.13	6.42	7.72
Metasediments (ms)	TC (Ur)	447	1.85	23.49	5.79	3.27	9.06	12.33	15.61
	eU (ppm)		1.00	9.63	1.56	1.21	2.77	3.97	5.18
	eTh (ppm)		0.96	18.61	3.62	2.63	6.25	8.87	11.50
	k%		0.25	2.83	0.96	0.45	1.41	1.87	2.32
	eU/eTh		0.07	1.64	0.47	0.21	0.67	0.88	1.08
	eU/k		0.20	8.42	1.69	0.96	2.65	3.60	4.56
	eTh/k		1.17	11.42	3.70	1.42	5.12	6.54	7.97
Metavolcanics (mv)	TC (Ur)	1355	1.36	21.57	3.47	1.81	5.28	7.09	8.90
	eU (ppm)		0.01	11.95	0.89	0.61	1.50	2.10	2.71
	eTh (ppm)		0.63	17.40	2.33	1.28	3.61	4.89	6.18
	k%		0.15	2.40	0.54	0.30	0.84	1.14	1.44
	eU/eTh		0.04	1.31	0.40	0.17	0.57	0.74	0.91
	eU/k		0.19	11.95	1.83	1.01	2.85	3.86	4.88
	eTh/k		1.58	17.54	4.66	1.51	6.17	7.68	9.19
Intermediate to acid metavolcanics (mva)	TC (Ur)	581	1.97	22.78	6.05	3.46	9.51	12.97	16.42
	eU (ppm)		0.08	6.87	1.45	0.86	2.32	3.18	4.05
	eTh (ppm)		0.79	17.48	3.95	2.33	6.28	8.62	10.95
	k%		0.16	3.24	1.01	0.58	1.59	2.18	2.76
	eU/eTh		0.08	1.26	0.39	0.13	0.51	0.64	0.77
	eU/k		0.29	5.93	1.62	0.78	2.40	3.18	3.96
	eTh/k		1.78	10.31	4.23	1.31	5.54	6.85	8.16
Basic metavolcanics (mvb)	TC (Ur)	214	2.06	16.45	5.81	3.21	9.01	12.22	15.43
	eU (ppm)		0.03	5.02	1.49	0.86	2.35	3.21	4.07
	eTh (ppm)		0.83	11.02	3.60	2.12	5.72	7.85	9.97
	k%		0.28	2.43	0.97	0.52	1.49	2.01	2.52
	eU/eTh		0.16	1.13	0.45	0.19	0.64	0.83	1.01
	eU/k		0.27	3.54	1.64	0.63	2.27	2.90	3.53
	eTh/k		1.61	7.75	3.79	1.17	4.96	6.13	7.30
Quaternary	TC (Ur)	619	2.34	28.77	9.76	4.65	14.41	19.06	23.70
	eU (ppm)		0.20	11.10	2.24	1.45	3.69	5.14	6.59
	eTh (ppm)		1.40	23.29	5.83	3.30	9.13	12.43	15.73
	k%		0.30	3.61	1.73	0.73	2.46	3.20	3.93
	eU/eTh		0.08	0.95	0.39	0.11	0.49	0.60	0.71
	eU/k		0.37	4.20	1.31	0.55	1.86	2.40	2.95
	eTh/k		1.65	8.86	3.42	0.97	4.39	5.36	6.32
serpentinite (sp)	TC (Ur)	404	1.18	16.64	5.09	2.67	7.76	10.43	13.10
	eU (ppm)		0.08	4.80	1.35	0.75	2.10	2.85	3.59
	eTh (ppm)		0.21	12.14	3.13	1.65	4.78	6.43	8.09
	k%		0.11	2.74	0.85	0.47	1.32	1.79	2.27
	eU/eTh		0.06	3.47	0.48	0.28	0.76	1.05	1.33
	eU/k		0.32	6.67	1.81	0.86	2.67	3.53	4.39
	eTh/k		1.61	13.35	3.93	1.18	5.11	6.29	7.47
Trachyte (TR)	TC (Ur)	7	8.56	22.39	16.55	4.82	21.36	26.18	31.00
	eU (ppm)		1.87	5.69	3.92	1.42	5.34	6.76	8.18
	eTh (ppm)		8.98	18.80	14.30	3.86	18.16	22.02	25.88
	k%		1.14	2.57	2.00	0.49	2.49	2.98	3.47
	eU/eTh		0.21	0.30	0.27	0.03	0.30	0.33	0.36
	eU/k		1.53	2.22	1.91	0.29	2.20	2.49	2.78
	eTh/k		5.89	8.13	7.17	0.87	8.04	8.91	9.78

No., number of observations; Min., minimum value; Max., maximum value; X, arithmetic mean; S, standard deviation.

In the uranium anomaly maps (Figs. 7 & 8), the position and magnitude of the deviation from the mean for eU, eU/eTh and eU/K are presented. The absence of a symbol in (Figs. 7 & 8), usually means that one standard deviation of the mean was within the mapped gamma ray parameter. As for economic potential, a high eU abundance coinciding with high eU/eTh and eU/K ratios could have the most promising anomalies (red circle-like symbol in the three variables in (Figs. 7 & 8). Three areas of large groupings of elevated eU values coinciding with elevated eU/eTh and eU/K values are clearly shown in (Figs. 7 & 8).

Fig (8) clarifies the detected anomalous zone of G. Umm Naggat pluton with travers lines : 2580 and 2570 , where have elevated eU, eU/eTh and eU/K (Red circles in all variables) associated with the albite granite of the northern border of the Umm Naggat pluton .

Figs. (2-8) shows that these three significant anomalies correspond for the most part with the coarse-to-medium-grained biotite-granites. With regard to the Umm Naggat pluton (Fig. 6), the albitized granite is represented by a strongly altered zone varying in width from 50 m to 250 m and in length from up to 7 km (Gaafar, 2015). There are several alteration processes related to the albitized granite, such as albitization, greisenization, kaolinization and fluoritization (Gaafar, 2015). EL-AFANDY et al., 2000 concluded that the metasomatic zonal pattern is developed at the northern endocontacts of the alkali feldspar granite resulting into a gross enrichment in the elements of Zr, Hf, Nb, Ta, U and Th towards the roof albitized and greisenized apogranitic zones. While The Umm Bisilla area ranked in second order intems of significant of uranium enrichment, it was originated by small mineralization of quartz veins break through muscovite-albite apogranite which intruded into the hammamat sediments and volcanics (El Ramly et al. 1970). The third enrichment uranium zone is associated with G. El Unayji pluton (25°13' 30" N,34°7' 48"E).

The third way of defining anomalies is by examining the stacked profiles for regions of high eU, eU/eTh and eU/K values, indicating uranium enrichment over the other natural radioelements. Examination of the stacked profile (Figs. 9-14) for flight line 2570, 2580 ,2600 2610, 2390, and 2400 assigned in (Fig. 7, 8), shows high concentrations of eU, associated with a slight increase in eU/eTh and an appreciable increase in eU/K and eTh/K ratios corresponding to coarse- to medium grained biotite-granites.

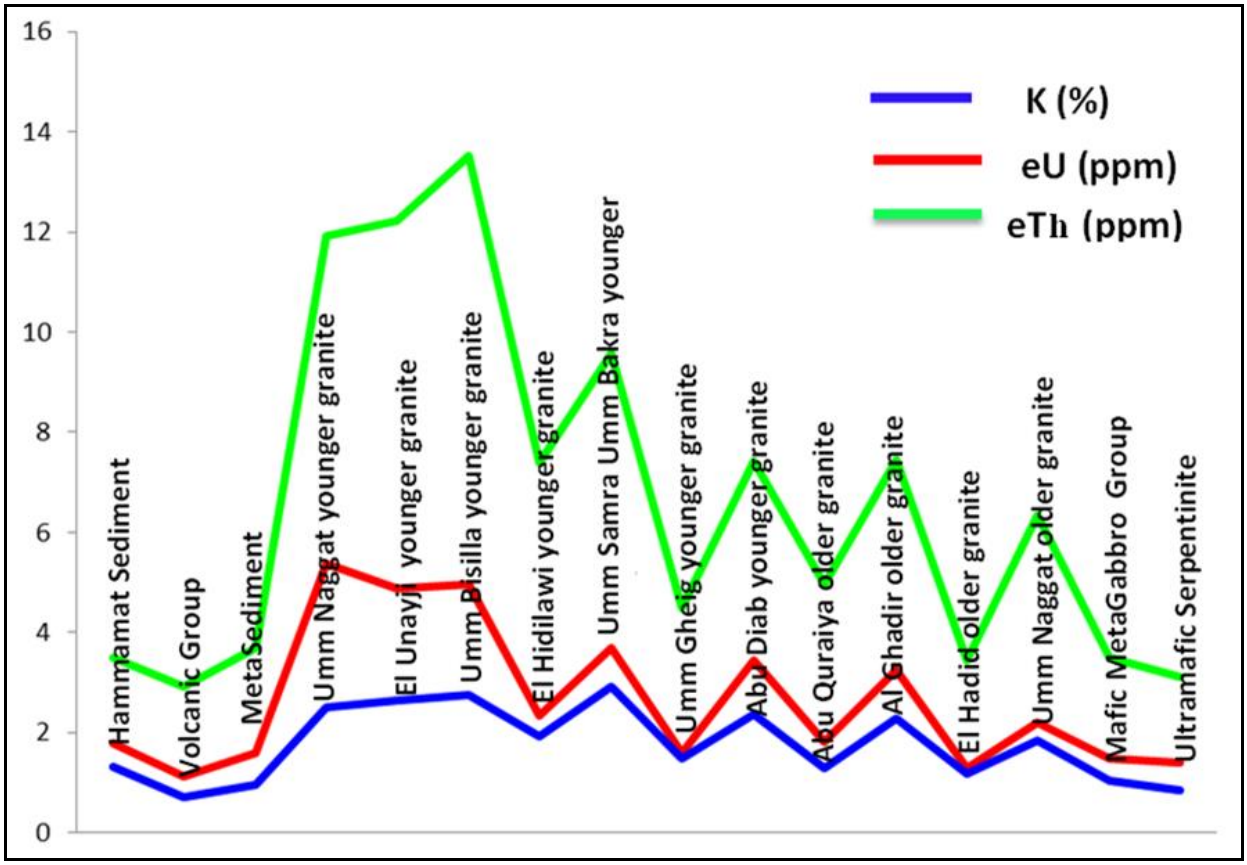

Fig. 9: Calculated background mean (X) of radioelements, for the different rock units of G. Umm Naggat area, Central Eastern Desert, Egypt.

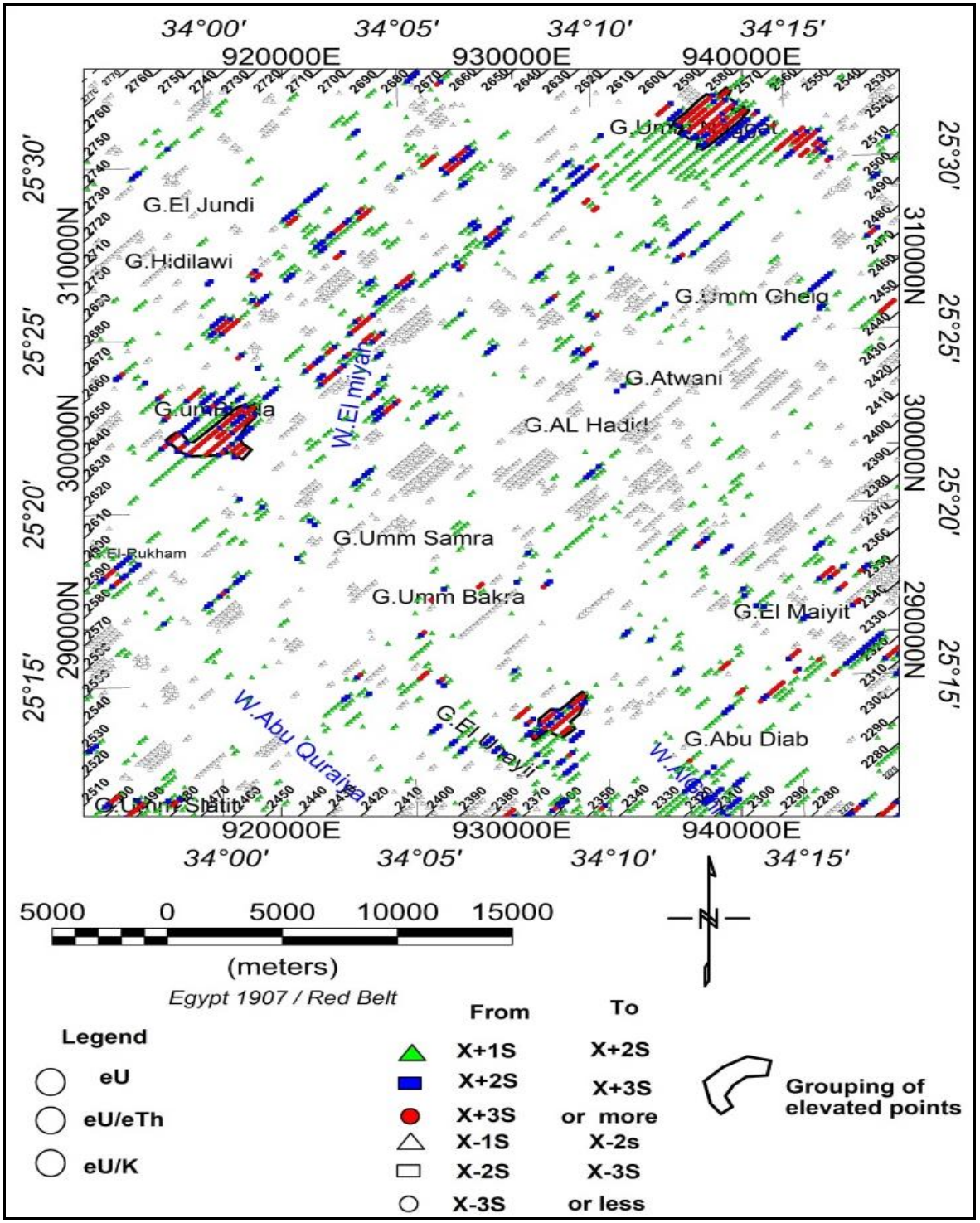

Fig. 10: The uranium point anomaly map, of G. Umm Naggat area, Central Eastern Desert, Egypt.

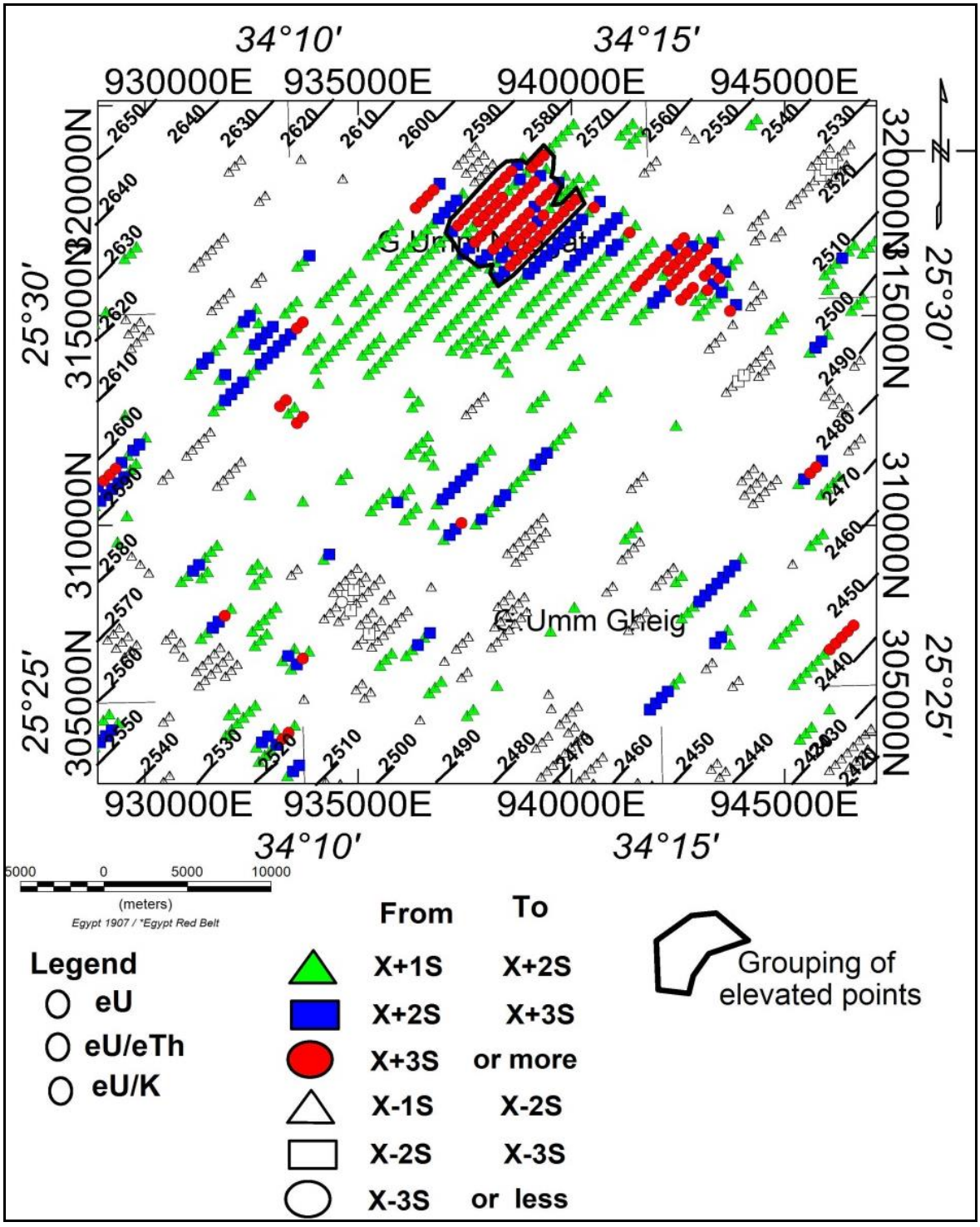

Fig. 11: Detailed point anomaly map of Anomalous Enrichment, of G. Umm Naggat pluton, Central Eastern Desert, Egypt.

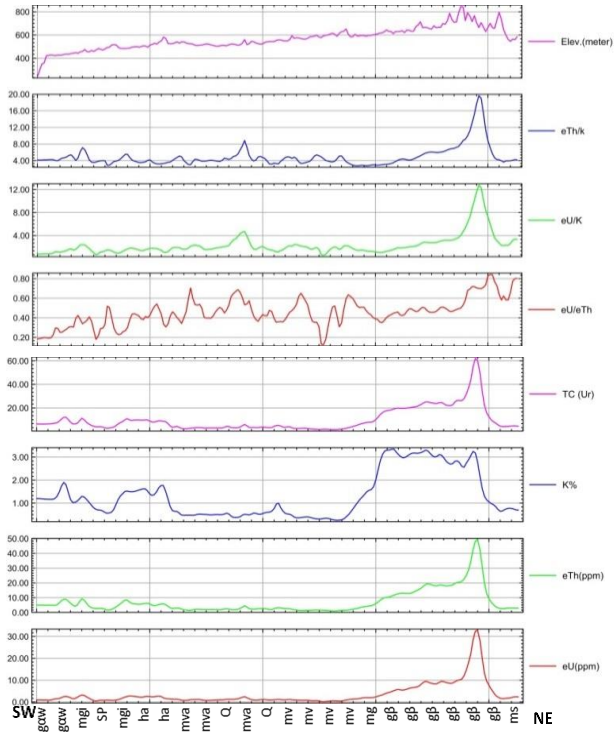

Fig. 12: Stacked Profile taken along flight line2570(After Aero Service, 1984). gα=older granite; gβW=Weathered younger granite; gβ=younger granite; mgi=intrusive metagabbro-diorite; mg=metagabbro-diorite; ms=metasedements; sp=serpentinite; Q=Quaternay ;mv: metavolcanics; mva: acedic metavolcanics; ha:hammamat sedemint.

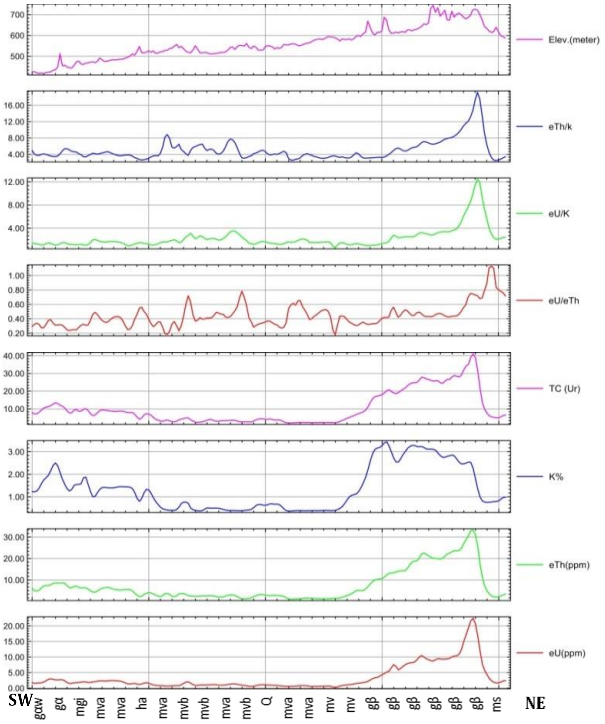

Fig. 13: Stacked Profile taken along flight line 2580(After Aero Service, 1984). gα= older granite; gβW=Weathered younger granite; gβ=younger granite; mgi=intrusive metagabbro-diorite; ms=metasedements; sp=serpentinite; Q=Quaternay ;mv: metavolcanics; mva: acedic metavolcanics; mvb: basic metavolcanics.

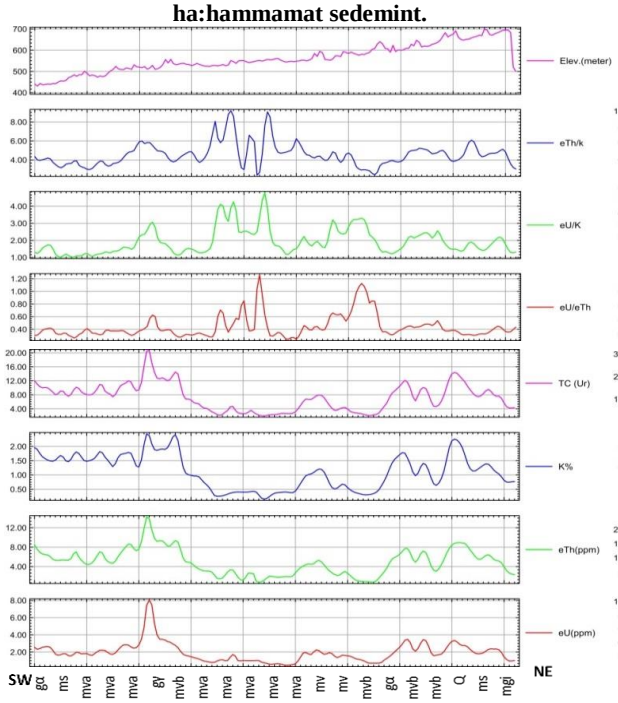

Fig.14:Stacked Profile taken along flight line 2600(After Aero Service, 1984). gα= older granite; gβW=Weathered younger granite; gβ=younger granite;gγ: coarse-grained biotite granite ; ms=metasedements; sp=serpentinite; Q=Quaternay ;mv: metavolcanics; mva: acedic metavolcanics; mvb: basic metavolcanics.

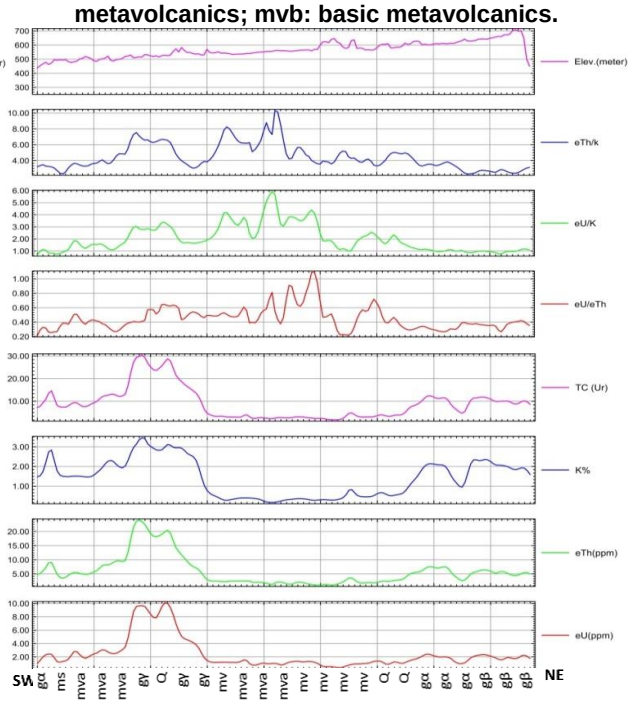

Fig.15:Stacked Profile taken along flight line 2610(After Aero Service, 1984). gα= older granite; gαW=Weathered older granite; gβ=younger granite; mg=metagabbro-diorite; ms=metasedements; sp=serpentinite; Q=Quaternay.

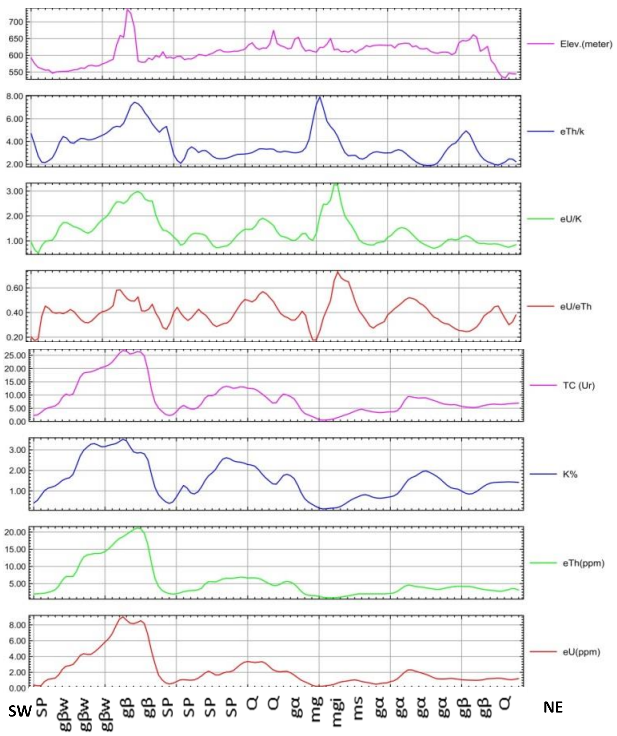

Fig. 16: Stacked Profile taken along flight line 2390 (After Aero Service, 1984).. gα= Older Granite; gβW=Weathered younger Granite; gβ=younger granite; mg=Metagabbro-diorite; ms=metasedements; sp=serpentinite; Q=Quaternay ;mvb:basic metavolcanics.

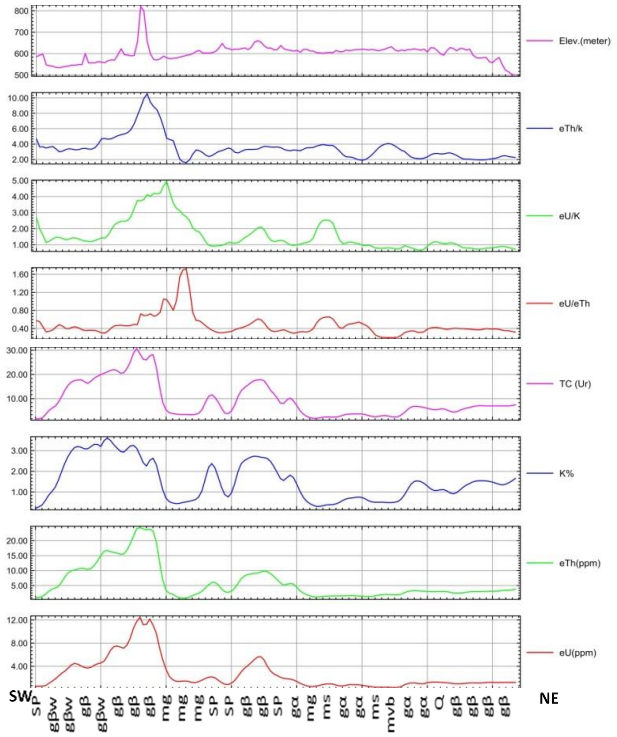

Fig. 17: Stacked profile taken along flight line 2400 (After Aero Service, 1984).. gα= Older Granite; gαW=Weathered Older Granite; gβ=younger granite; mg=Metagabbro-diorite; ms=metasedements; sp=serpentinite; Q=Quaternay;mvb:basic metavolcanics.

4. CONCLUSIONS

From the current study, several point can be concluded :

(1) An exploration of gamma ray spectrometric surveys over broad regions, like the Eastern Desert of Egypt, help to outline uraniferous provinces. So, it is possible to apply more detailed methods of prospecting to the most promising areas.

(2) The statistical treatment of spectrometric gamma ray data broad regions reveals three locations of abnormally elevated points found on the uranium anomaly map. They are associated with medium-grained granites and represent the most promising gamma ray spectrometric anomalies in the Umm Naggat area . Generally, it can be concluded from similar cases that attention can be restricted to these localities and that the area to be ground searched can be reduced substantially.

REFERENCES

Abd El Nabi, S.H., (1995). Statistical evaluation of airborne gamma ray spectrometric data from the Magal Gebriel area, south Eastern Desert, Egypt. Journal of Applied Geophysics 34 (1995) 47-54.

Aero-Service (1984). Final operational report of airborne magnetic radiation survey in the Eastern Desert, Egypt for the Egyptian General Petroleum Corporation. AeroService, Houston, Texas, Six Volumes.

Conoco Coral, (1987): Geological map of Egypt, scale 1:500,000.

EL-AFANDY, A., Abdalla, H.D., Aly, M.M. and Ammar, F. (2000). Geochemistry and Radioactive Potentiality of Um Naggat Apogranite, Central Eastern Desert, Egypt, RESOURCE GEOLOGY, vol. 50, no. 1, 39–51, 2000.

El-Ramly M, Ivanov S, Kochin G (1970). Tin-tungsten mineralization in the Eastern Desert of Egypt. In: Studies on some mineral deposits of Egypt. The Egyptian geological survey, Cairo, pp 43–52.

Gaafar, I., (2015). Integration of geophysical and geological data for delimitation of mineralized zones in Um Naggat area, Central Eastern Desert, Egypt. NRIAG Journal of Astronomy and Geophysics (2015), http://dx.doi.org/10.1016/ j.nrjag.2015.04.004.

International Atomic Energy Agency (IAEA), (1979). Gamma Ray Surveys in Uranium Exploration. IAEA, Vienna, Techn. Rep. Ser., 186,90 pp.

Sabet, A.H., (1961). Geology and mineral deposits of G. El-Sibai area, Red Sea hills, Egypt, UAR: D.Sc. Thesis, Leiden State University, The Netherland. 188 p.

Sabet, A.H., V.V.Bessonenko and B.A. Bykov (1976). The intrusive complexes of the Central Eastern Desert of Egypt. Ann. Geol. Surv.Egypt.6: pp. 53-73.

Saunders, D.F. and Potts, M.J., (1976). Interpretation and application of high sensitivity airborne gamma ray spectromettic data. In: IAEA Symp. Exploration for Uranium Ore Deposits, Vienna, pp. 107-124.